

Supplementary Material for

Calibration of mercury analyzers: Assessment of agreement between four methods

Youngchul Byun,^a Dong Nam Shin,^{b,} Sung-Won Ham,^c Kyung Lee^d*

^aSchool of Chemical Engineering and Analytical Science, The University of Manchester

^bEnvironmental Research Department, Research Institute of Industrial Science & Technology

^cDepartment of Display & Chemical Engineering, Kyungil University

^dDS Science Company

*Corresponding author telephone: +82-54-279-6540; fax: +82-54-279-6239; e-mail: jydnshin@rist.re.kr

Contents

Contents	Title	Page
Text	Effect of gases passing through the mercury saturator	S2
Fig. S1	Effect of gases passing through the mercury saturator on the generation of Hg ⁰ .	S3
Text	Effect of the water condensation unit on the Hg ⁰ signal	S4
Fig. S2	Effect of the water condensation unit on the Hg ⁰ signal when a mercury solution was used for calibration.	S4
Text	Illustration of Hg solution method	S5
Fig. S3	Output signal obtained from the use of Hg solution.	S6
Text	Illustration of UV method using Beer's law	S7
Fig. S4	Use of the absorption coefficient of Hg ⁰ at 253.7 nm light employing Beer's law.	S8
Table S1	Data obtained from the UV absorption coefficient method	S9
Text	Antonie, Wagner, and Dumarey equations	S10
Table S2	Coefficients (a _i) and their standard deviations	S10
Table S3	Fixed parameters (T _c and P _c)	S11

Effect of gases passing through the mercury saturator

If the effluent Hg^0 has been saturated at each temperature of the mercury saturator, the increase in the Hg^0 signal in the mercury saturator must be stopped at 10 °C because the temperature of the condensation vessel was also set to 10 °C. This means that the mercury saturator cannot emit saturated Hg^0 controlled by the temperature. This is believed to be caused by the gases passing through the mercury saturator. Therefore, this study examined the effect of the flow rate of gases passing through the mercury saturator on the Hg^0 concentration. The temperature of the mercury saturator was set to 10 °C and the flow rates of N_2 passing through the mercury saturator were increased from 10 to 300 mL min^{-1} . Finally, it was diluted with N_2 . The total flow rate was fixed to 2 L min^{-1} (Fig. S1). If the flow rate cannot affect the saturation of Hg^0 inside the mercury saturator, the data obtained must be the dashed line in Fig. S1. However, with increasing flow rate, a larger deviation can be found between the assumed and practical data. This means that the precise concentration of Hg^0 is difficult to obtain with the gases passing continually through the mercury saturator. Therefore, two-stage mercury vapor control is essential for a steady injection of precise Hg^0 for the method using the vapor pressure of mercury.

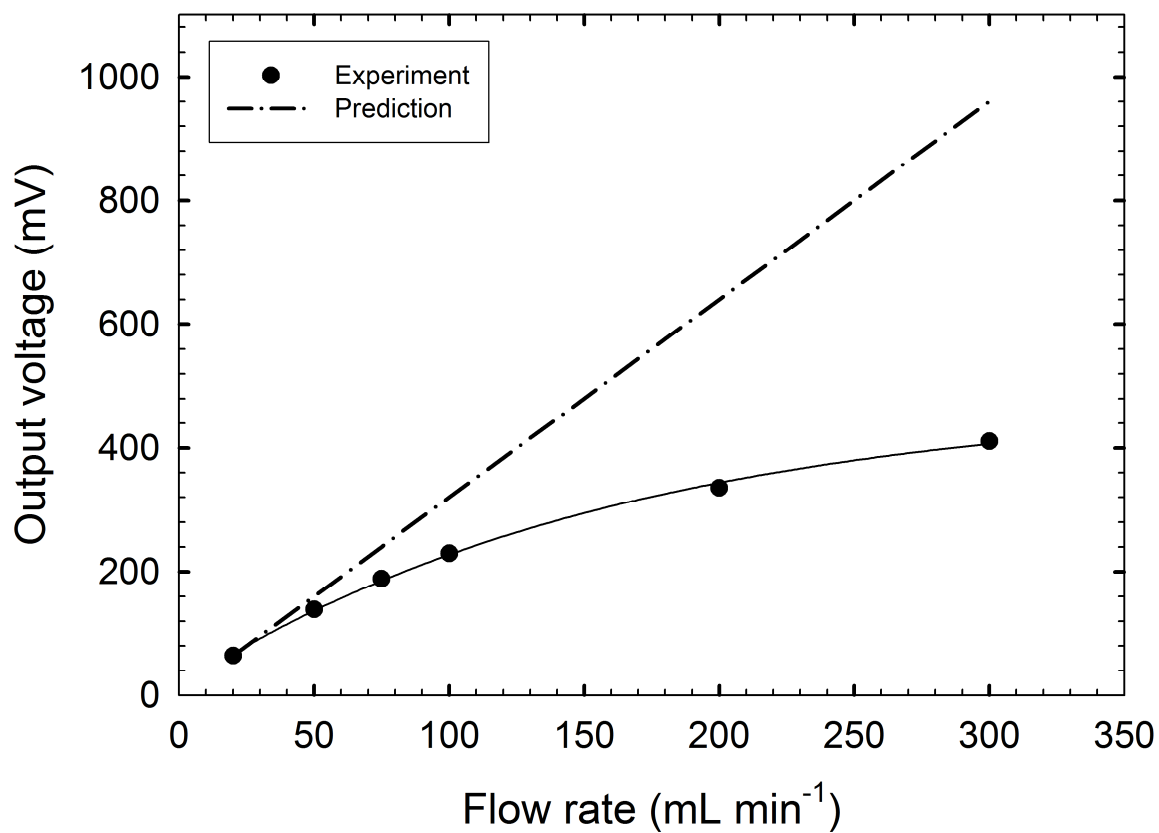


Fig. S1. Effect of gases passing through the mercury saturator on the generation of Hg^0 .

Experimental conditions: temperature of mercury saturator = 10 °C, total flow rate (gases passing through the mercury saturator + dilution gases) = 2 L min⁻¹. The dash line was calculated based on the Hg^0 signal of 20 ml gases passing through the mercury saturator.

Effect of the water condensation unit on the Hg^0 signal

The effect of the water condensation unit on the Hg^0 signal was examined by initially introducing Hg^0 in the N_2 balance using a permeation tube into the moisture condensing unit without a water bubble and then turning the pass line of Hg^0 into the impinger containing distilled water (Fig. S2). The results revealed little effect on the Hg^0 concentration.

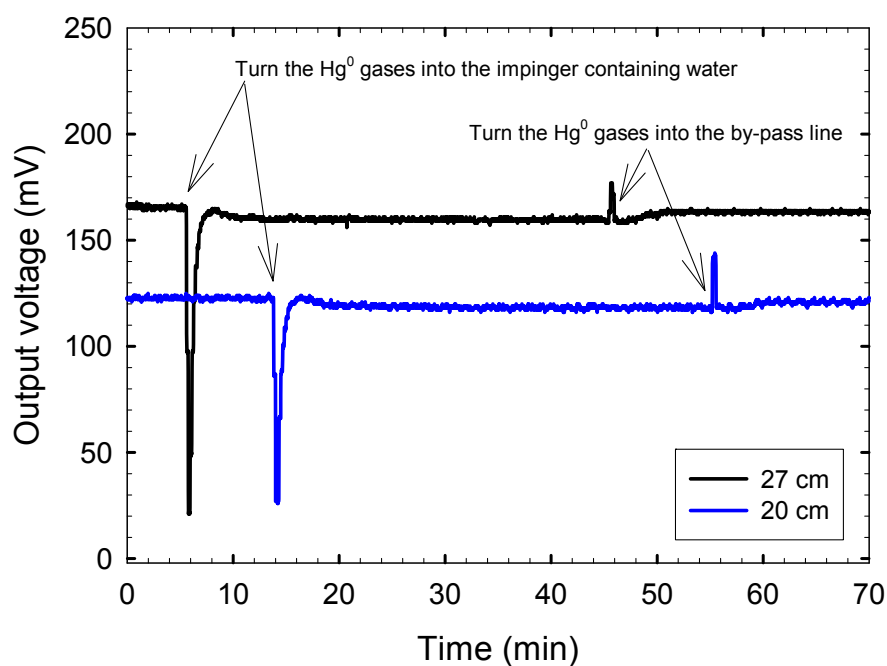


Fig. S2. Effect of the water condensation unit on the Hg^0 signal when a mercury solution was used for calibration. Initially, only N_2 containing Hg^0 was introduced into the CVAAS via the moisture condensing unit. Subsequently, the gas flow was passed through the impinger containing mercury.

Illustration of Hg solution method

Two parameters (flow rate of passing N₂ and the amount of Hg dissolved in water) were changed and the area of peak signal of Hg⁰ was calculated. The area of the signal increased and decreased with increasing amount of the Hg contained in the solution and flow rate of aerated N₂, respectively (Fig. S3).

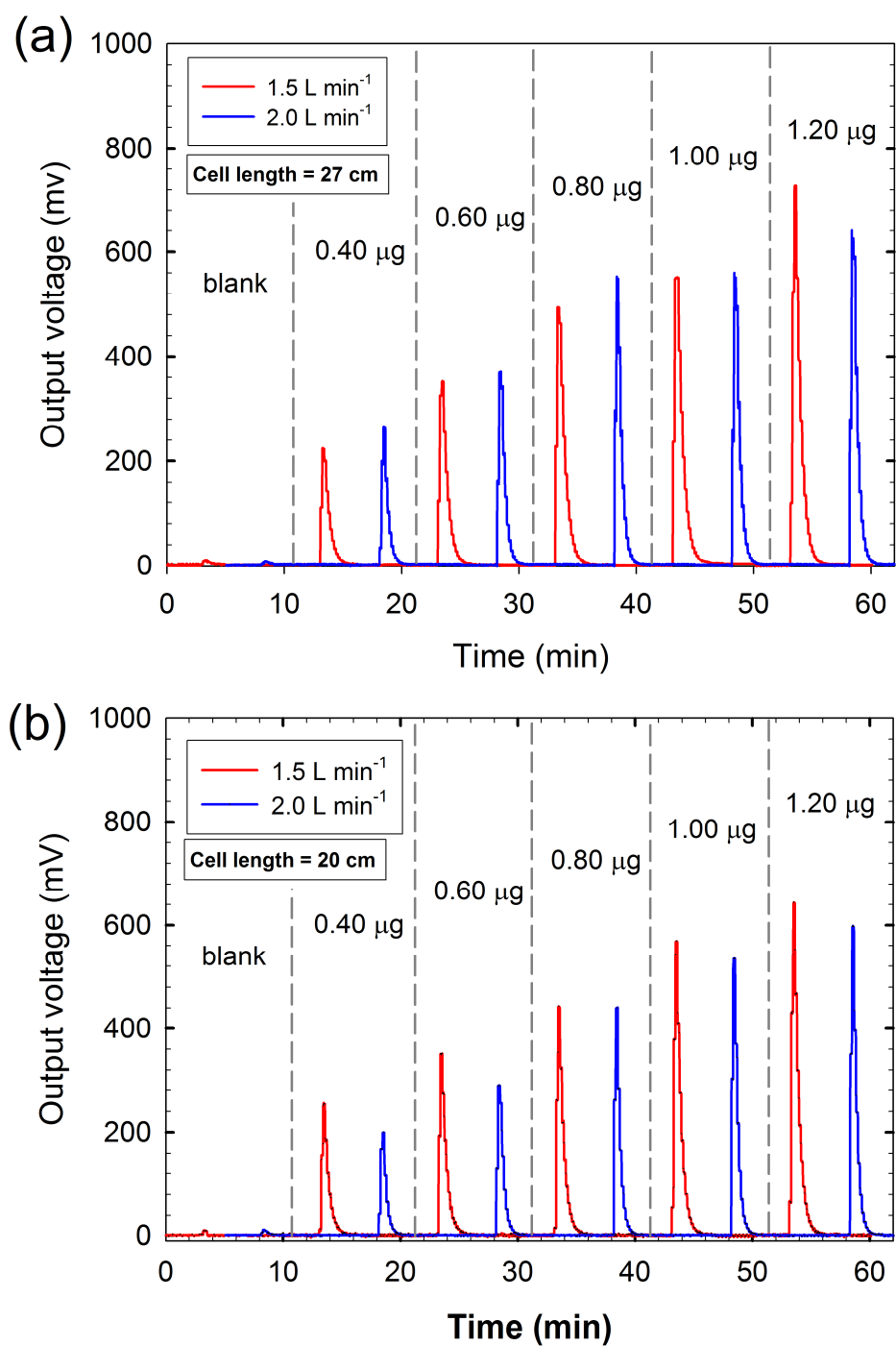


Fig. S3. Output signal obtained from the use of Hg solution. (a) 27 cm of the cell length.

(b) 20 cm of the cell length. The small peaks in blank originated from the traces of the used reagents.

Illustration of UV method using Beer's law

Initially, the response of CVAAS as a function of the calculated Hg^0 concentration using the permeation tube was obtained according to the cell length (Fig. S4(a)). $\ln(I/I_0)$ (Fig. S4(b)) was calculated and redrawn as a function of the cell length of CVAAS (Fig. S4(c) of SI). At each fit in Fig. S4, the slope and deviation was obtained (Table S1). The slope of Fig. S4(c) is a function of the absorption coefficient and Hg^0 ($-kC_{\text{Hg}}$) concentration. Therefore, the Hg^0 concentration was obtained using the absorption coefficient (k) and slope. Finally, the concentration calculated from the slope of Fig. S4(c) was compared with the concentration calculated from the injected Hg^0 using a permeation tube (Fig. S4(d)). Finally, using the ratio of the concentration calculated from the absorption coefficient to the permeation tube, the increment, α_{UV} , was determined to be and 0.0868 and 0.0653 for 20 cm and 27 cm cells, respectively.

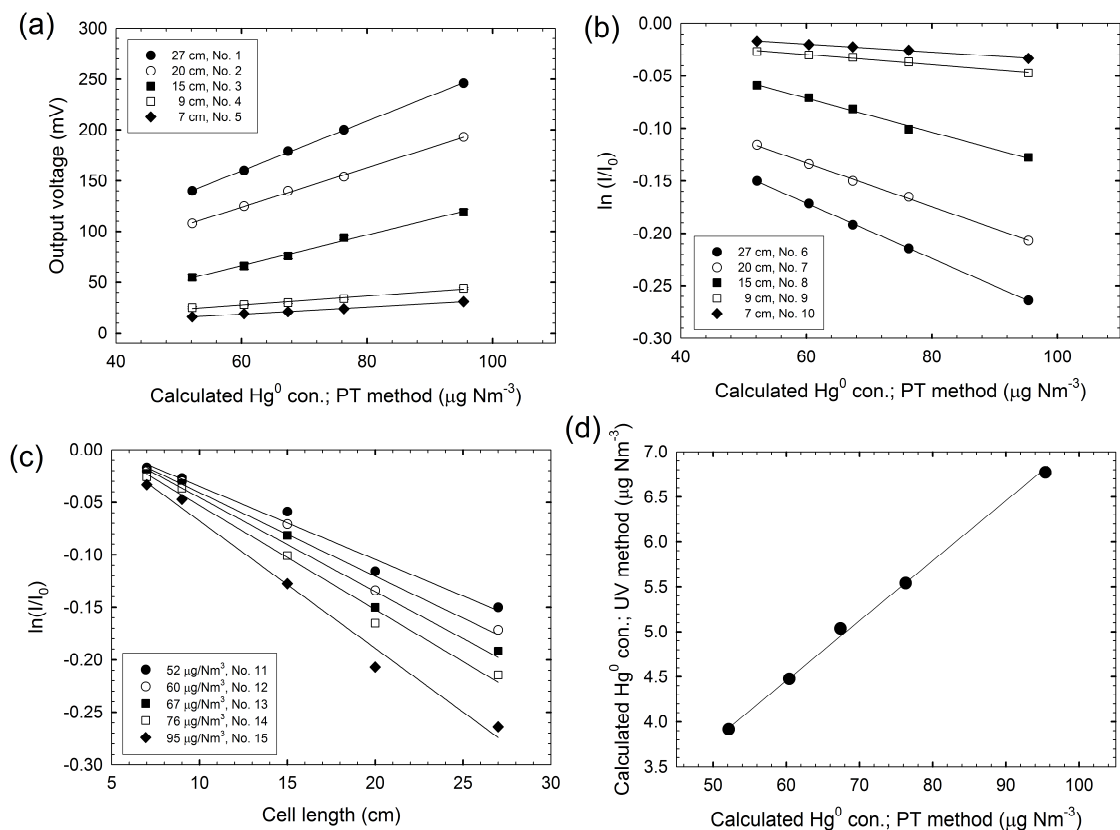


Fig. S4. Use of the absorption coefficient of Hg^0 at 253.7 nm light employing Beer's law. (a) The output signal of the CVAAS as a function of the injected Hg^0 concentration. The concentration of injected Hg^0 was determined using a permeation tube. (b) $\ln(I/I_0)$ converted from Fig. S4(a). (c) Redrawn graph using Fig. S4(b) as a function of the cell length. (d) Calculated Hg^0 concentration as a function of the injected Hg^0 concentration obtained the permeation tube.

Table S1. Data obtained from the UV absorption coefficient method

Number	Fitted equation	R ²	Calculated Hg concentration ($\mu\text{g Nm}^{-3}$)
No. 1	$Y=2.4537x + 12.4312$	1.0000	-
No. 2	$Y=1.9455x + 7.1715$	0.9999	-
No. 3	$Y=1.5130x - 24.4086$	0.9996	-
No. 4	$Y=0.4408x + 1.1953$	0.9995	-
No. 5	$Y=0.3334x - 2.0222$	0.9999	-
No. 6	$Y=-0.0026x - 0.0133$	1.0000	-
No. 7	$Y=-0.0021x - 0.0077$	0.9999	-
No. 8	$Y=-0.0016x - 0.0262$	0.9996	-
No. 9	$Y=-0.0005x - 0.0013$	0.9995	-
No. 10	$Y=-0.0004x + 0.0022$	0.9999	-
No. 11	$Y=-0.0070x + 0.0349$	0.9935	3.9
No. 12	$Y=-0.0080x + 0.0390$	0.9940	4.5
No. 13	$Y=-0.0090x + 0.0441$	0.9945	5.0
No. 14	$Y=-0.0099x + 0.0461$	0.9968	5.5
No. 15	$Y=-0.0121x + 0.0536$	0.9962	6.8

Antonie, Wagner, and Dumarey equations

The Antonie equation is as follows,

$$\log P_{sat} [mmHg] = A - \frac{B}{T[K]},$$

where A is a constant equal to 7.871936 and B is a constant equal to 3143.28.

The Wagner equation is as follows,

$$\ln\left(\frac{P}{P_c}\right) = \left(\frac{T_c}{T}\right)(a_1\tau + a_2\tau^{1.89} + a_3\tau^2 + a_4\tau^8 + a_5\tau^{8.5} + a_6\tau^9), \quad \tau = 1 - \frac{T}{T_c},$$

where coefficients (a_i) and their standard deviations are given in Table S2 and fixed parameters (T_c and P_c) are given in Table S3.

Table S2. Coefficients (a_i) and their standard deviations

i	a_i	Std.dev.
1	-4.57618368	0.0472
2	-1.40726277	0.8448
3	2.36263541	0.8204
4	-31.0889985	1.3439
5	58.0183959	2.4999
6	-27.6304546	1.1798

Table S3. Fixed parameters (T_c and P_c)

T_c (K)	P_c (MPa)
1764	167

The Dumarey equation is as follows,

$$\gamma_{Hg} = \frac{D}{T} 10^{-(A + [B/T])},$$

where γ_{Hg} is the mass concentration of saturated mercury in the air inside the calibration vessel, in ng ml^{-1} , T is the temperature of the air inside the calibration vessel, in K, A is a constant equal to -8.134459741 , B is a constant equal to 3240.871534 K, and D is a constant equal to 3216522.61 K ng ml^{-1} .